JOURNAL OF AGRICULTURAL AND FOOD CHEMISTRY

Atomic Force Microscopy Studies on Heat-Induced Gelation of Curdlan

SHINYA IKEDA* AND YUKA SHISHIDO

Department of Food and Human Health Sciences, Osaka City University, 3-3-138 Sugimoto, Sumiyoshi-ku, Osaka 558-8585, Japan

Heat-induced gelation of a cold-water insoluble polysaccharide, Curdlan, was investigated using atomic force microscopy (AFM). Curdlan dissolved into NaOH aqueous solutions exhibited a spectral transition around 0.2 mol/L NaOH, which is an indicative of conformational transitions from a single helix at a lower alkali concentration to a disordered chain at a higher concentration. Nevertheless, AFM images of Curdlan solubilized in 0.01 mol/L NaOH revealed the presence of heterogeneous supramolecular assemblies of Curdlan: the majority of the molecules were in the form of microfibrils, the lengths of which were on the order of micrometers and the cross-sectional heights of which were ∼2−3 nm, whereas single molecular chains, partially dissociated from these microfibrils, were also observed. Heating such a sol resulted in the formation of densely cross-linked microgel networks. Heat-induced gelation of Curdlan appears to be initiated by partial dissociation of single chains from supramolecular microfibrils and followed by cross-linking of microfibrils via hydrophobic interactions among these partially dissociated chains.

KEYWORDS: Curdlan; microbial polysaccharide; single helix; triple helix; hydrophobic interactions; heat-induced gel; atomic force microscopy

INTRODUCTION

Gel-forming polysaccharides are widely used in the food industry because their abilities to provide the whole range of viscoelastic properties are indispensable for obtaining the desired stability, structure, and/or textural properties of products (*1*). Many polysaccharides such as agar (agarose), carrageenans, and gellan form a gel on cooling via coil-to-helix conformational transitions, whereas those that form a gel on heating are also known (*2*, *3*). Curdlan, a microbial exopolysaccharide composed entirely of 1→3-linked β-D-glucopyranoses, is among such heat-gelling polysaccharides (*4*−*7*). In addition to the application as a texture modifier, strong antitumor and immune-stimulatory activities of (1→3)-β-glucans in general have been attracting attention and have utility as food additives (*8*−*10*).

Curdlan is insoluble in water at an ambient temperature, but its aqueous suspension may form a gel on heating. Two types of heat-induced Curdlan gels have been recognized and traditionally referred to as low-set and high-set gels (*11*). A low-set gel can be obtained by heating an aqueous suspension of Curdlan to ∼55−65 °C and subsequently cooling it to ambient temperatures. A high-set gel can be formed on heating at a higher temperature, typically >80 °C. A low-set gel melts on reheating, whereas a high-set gel is stable against subsequent thermal processing such as freezing and retorting, making this type of Curdlan gel an effective material for controlling the physical properties of food products (*12*). However, the exact molecular mechanism of heat-induced gelation of Curdlan remains largely unclear due to its insolubility into cold water. Dried Curdlan powder particles suspended in water swell on heating to 55−65 °C by absorbing water. At this stage of heating, only a limited number of Curdlan molecules are believed to be molecularly solubilized (*7*). Therefore, a low-set gel may be regarded as an assembly of packed cohesive swollen particles, interacting via hydrogen bonding, whereas hydrophobic interactions should be involved in the high-set gelation.

Three reported conformational states of Curdlan are triple-stranded helix, single-stranded helix, and disordered single chain (*13*, *14*). Commercially available Curdlan occurs as imperfectly crystalline granules because its manufacturing processes include solubilization using strong alkali and drying (*7*). Early X-ray fiber diffraction studies have reported that an annealed form of Curdlan crystallizes as a triple-stranded helix in a hexagonal unit cell with the base-plane dimension of 1.44 nm (*13*). The triple-helix structure is believed to denature to yield individual disordered single chains in alkaline aqueous solutions or organic solvents such as dimethyl sulfoxide (DMSO) (*15*, *16*). Solid-state ^{13}C NMR studies have concluded that hydrated Curdlan molecules prepared from commercially produced spray-dried powders predominantly adopt single-helical conformation and that heating at high temperatures causes hydrophobic association of the single helices as well as transformation of single helices into triple helices to a limited degree (*14*). Associated single helices and triple-helical parts are considered to be able to play

* Author to whom correspondence should be addressed (telephone +81-6-6605-2862; fax +81-6-6605-3086; e-mail ikeda@life.osaka-cu.ac.jp).

10.1021/jf048797r CCC: $30.25
Published on Web 01/14/2005

a role as junction zones in network structure on the assumption that a single molecular chain can be involved in more than one junction zone.

Structures in supramolecular assemblies of Curdlan have been investigated mainly using electron microscopy (*17*−*21*). Transmission electron microscopy (TEM) images of negatively stained specimens prepared from both unheated and heat-treated Curdlan dispersions reveal network structures composed of entangled microfibrils, the width of which is 10−20 nm without heat treatments and increases to 30−40 nm by heating at 120 °C (*18*). Atomic force microscopy (AFM) is an alternative microscopy method that allows direct observation of unstained biopolymers and their assemblies at a high-resolution comparable to or even better than TEM in optimum conditions (*22*−*24*). AFM has been successfully utilized to visualize polysaccharide microgels produced in aqueous sols (*25*, *26*) as well as the surface of bulk polysaccharide gels submerged in aqueous solutions of salts (*27*). An additional advantage of AFM over TEM is that it provides quantitative information of heights of objects in an image. The purpose of this study was to directly visualize molecular and supramolecular structures in unheated and heat-treated Curdlan using AFM in order to gain insight into the mechanism of the heat-induced assembling phenomenon of this water-insoluble polysaccharide.

MATERIALS AND METHODS

Materials. Spray-dried Curdlan powder (lot DL-15A) was supplied by Takeda Chemical Industries, Ltd. (Osaka, Japan). A reagent grade Congo Red and sodium hydroxide were purchased from Kanto Chemical Co., Inc. (Tokyo, Japan), and Wako Pure Chemical Industries, Ltd. (Osaka, Japan), respectively. Weighed amounts of Curdlan powders were dispersed into 0.01−1 mol/L NaOH aqueous solutions in nitrogen atmosphere to be 1% w/w and moderately stirred using a magnetic stirrer overnight (15 h) at room temperature. Portions of the Curdlan solutions containing 0.01 mol/L NaOH were heated at 90 °C until remarkable structural changes were detected using AFM. Congo Red was dissolved into distilled water to be 0.03 mmol/L.

Visible Absorption Spectroscopy. Equal volumes of the Congo Red solution and distilled water, NaOH aqueous solutions, or the above-prepared Curdlan solutions containing NaOH were mixed thoroughly. Visible absorption spectra of these mixed solutions were immediately recorded at room temperature using a UV−vis spectrophotometer (UVmini-1240, Shimadzu, Kyoto, Japan) in the wavelength range of 400−600 nm. Sample preparation and measurements were at least triplicated, and averaged values of data are reported with estimated errors.

Atomic Force Microscopy. Small amounts (0.1−0.3 mL) of the unheated and heated 1% w/w Curdlan solutions containing NaOH were diluted into 50 mL of distilled water or 1 mol/L NaOH. Aliquots (2 μL) of the diluted samples were immediately spread onto freshly cleaved mica surfaces, air-dried, and imaged by AFM in air. AFM imaging was made at room temperature using an alternating current (ac) cyclic contact mode of a multimode imaging unit (SPA-400, Seiko Instruments Inc., Chiba, Japan) equipped with a controller (SPI3800N, Seiko Instruments Inc.). Samples were placed on top of the piezoelectric scanner, the maximum *xy* imaging range of which is ∼20 μm, and scanned at a scanning frequency of 0.5−1 Hz using a beam-shaped Si cantilever with a quoted spring constant of 12 N/m at a driving frequency of 136 kHz. Sample preparation was at least triplicated, and approximately 10−50 images were taken for each preparation.

RESULTS AND DISCUSSION

Molecular characterization of Curdlan can be hampered by its insolubility in water at ambient temperatures. Among known solvents of Curdlan, dilute aqueous solutions of alkali are relatively harmless, compared to other organic solvents such as DMSO or cadmium-containing cadoxen in which even cellulose is soluble. Additionally, heat-induced gels prepared from alkaline-solubilized Curdlan are fairly transparent and thus suitable for physicochemical characterization such as light or X-ray scattering studies (*4*, *5*). When solubilized in a dilute alkaline solution, Curdlan is believed to adopt a single-helical conformation (*14*). It has been reported that Curdlan single helices form a complex with an acid−base indicator, Congo Red, in dilute alkaline solutions, providing a simple method for detecting their presence (*28*−*31*). **Figure 1** shows relationships between the concentration of sodium hydroxide and the peak wavelength at which the absorption of Congo Red reaches its maximum in the wavelength range of 400−600 nm. In the presence of Curdlan, the peak wavelength shifted from ∼515−520 to ∼485−490 nm at the NaOH concentration slightly above 0.2 mol/L with increasing alkali concentration. These results are consistent with previous papers (*28*−*31*) and considered to reflect the conformational transition of Curdlan from a single helix to a disordered random coiled conformation occurring around 0.2 mol/L NaOH with increasing alkali concentration.

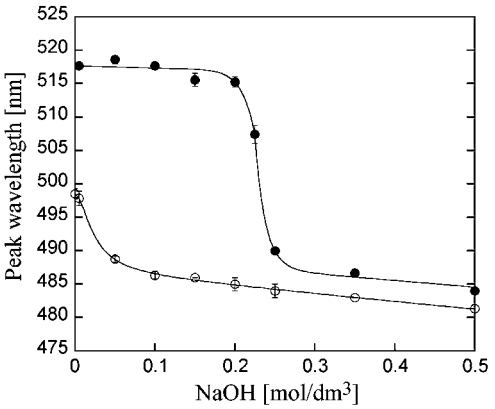

Figure 1. Alkali concentration dependence of the wavelength at the absorption maximum of Congo Red (peak wavelength) in the presence (●) and absence (○) of Curdlan.

Figure 2 shows AFM images of Curdlan deposited onto the freshly cleaved mica surface from a 0.6 mg/mL sol that has been diluted into distilled water from a 1% w/w sol in 0.01 mol/L NaOH. It has been reported that similar preparation conditions result in a fairly uniform single-layer coverage of polysaccharide molecules on the mica surface as long as they are sufficiently solubilized (*22*, *23*, *25*−*27*). However, **Figure 2a** reveals discrete network-like structures. The heights of microfibrils comprising these networks greatly vary but are typically in the range of a few nanometers (**Figure 2b**). These values are significantly larger than the reported dimension of the unit cell base plane of a triple-helix Curdlan crystal (1.44 nm) (*13*), suggesting that the observed microfibrils are composed of laterally associated bundles of Curdlan molecules. At higher magnification, variations in height or thickness of individual fibrils can be clearly seen (**Figure 2c**). The heights of thick fibrils exceed 3 nm (**Figure 2d**), whereas those of the finest fibrils are <1 nm (**Figure 2e**). These results provide the first direct evidence for the structural heterogeneity in molecular assemblies of Curdlan. The fine fibrils are considered to be single molecular chains of Curdlan, although no X-ray crystallographic data of single-helical Curdlan are available in the literature as far as we are aware. It is also worth noting that there is always a possibility that AFM-measured heights are underestimated because objects may be vertically compressed by the contacting probe tip (*32*). In the present case, Curdlan was first dissolved into 0.01 mol/L NaOH and then diluted

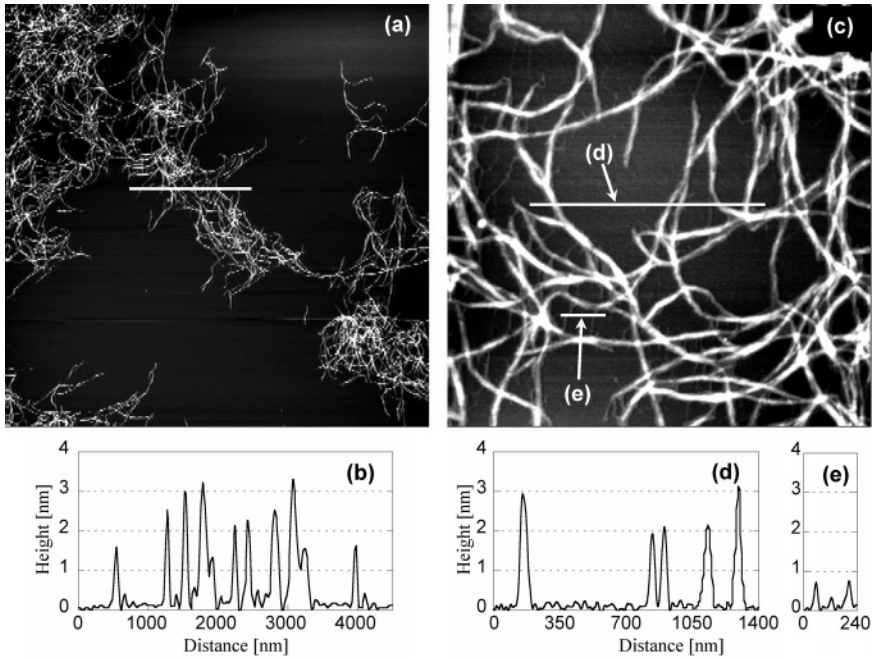

Figure 2. Topographical images of Curdlan dissolved into 0.01 mol/L NaOH to be 1% w/w, diluted into distilled water to be 0.6 mg/mL, and deposited onto mica. (**a**) Image size is 15 μm × 15 μm. (**b**) Height profile of the cross section highlighted in image **a**. (**c**) Image size is 2.5 μm × 2.5 μm. (**d**, **e**) Height profiles of the cross sections highlighted in image **c**.

into distilled water. Thus, even if Curdlan molecules are molecularly solubilized in 0.01 mol/L NaOH, decreased alkali concentration by dilution in water may cause a certain degree of intermolecular reassociation. In fact, recent static light-scattering studies have shown that the molecular association of Curdlan progresses with decreasing NaOH concentration in the range of 0.01−0.1 mol/L (*4*). Further intermolecular association is then likely to occur during the following air-drying operation after deposition on mica because of an increased polysaccharide concentration. This network formation process may be parallel to that of low-set gelation, involving partial solubilization by moderate heating and molecular association via hydrogen bonding on successive cooling.

The solubility of Curdlan was further investigated by dissolving into 1 mol/L NaOH. At this level of alkali, Curdlan should be completely solubilized and in the conformation of disordered random coils on the basis of the results shown in **Figure 1**. **Figure 3** is an AFM image of Curdlan deposited on mica from a 0.2 mg/mL sol that has been diluted into 1 mol/L NaOH from a 1% w/w sol with 1 mol/L NaOH. Observation of Curdlan molecules in this condition was very much limited because most areas on the mica surface were covered with alkali solids precipitated during drying. It was still possible to find unburied Curdlan molecules in the vicinity of precipitates. **Figure 3** reveals entangled and branched microfibrils, similar to those shown in **Figure 2**. The heights of microfibrils greatly vary, typically ranging from 0.5 to 3 nm. These results indicate that at least a part of Curdlan molecules are not molecularly solubilized even in 1 mol/L NaOH. If this is indeed the case, even more microfibrils should remain insoluble in dilute alkaline solutions such as 0.01 mol/L NaOH. Additionally, it is difficult to exclude the possibility that not only single helices but also triple-stranded helices originating from the native form are preserved within the observed microfibrils. Spectroscopic properties such as those shown in **Figure 1** are perhaps dominated by the majority of solubilized molecules, whereas rheological properties that are quite sensitive to the presence of polymer aggregates (*26*) could be influenced by the presence

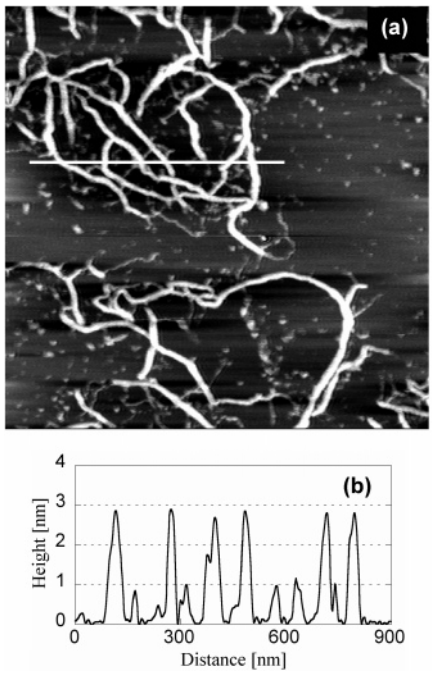

Figure 3. (**a**) Topographical image of Curdlan dissolved into 1 mol/L NaOH to be 1% w/w, diluted into 1 mol/L NaOH to be 0.2 mg/mL, and deposited onto mica. Image size is 1.5 μm × 1.5 μm. (**b**) Height profile of the cross section highlighted in image **a**.

of a small number of insoluble microfibrils. The present results highlight the advantage of microscopy that directly visualizes heterogeneity in the sample over other biophysical characterization techniques that provide results spatially averaged over an enormous number of molecules. AFM is particularly advantageous in terms of resolution in comparison with TEM that requires elaborate sample preparation procedures such as negative staining.

Figures 4 and **5** represent images of Curdlan heated at 90 °C for 4 h in 0.01 mol/L NaOH before being diluted and

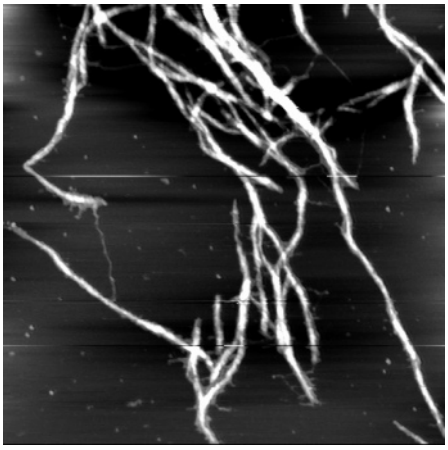

Figure 4. Topographical image of heat-treated Curdlan deposited onto mica. Curdlan was first dissolved into 0.01 mol/L NaOH to be 1% w/w, heated at 90 °C for 4 h, diluted into distilled water to be 0.2 mg/mL, and deposited onto mica. Image size is 2.5 μm × 2.5 μm.

deposited on mica. Two types of supramolecular assemblies were reproducibly observed after the heat treatment. The more commonly observed structure was branched microfibrils with partially dissociated single chains (**Figure 4**), similar to the images shown in **Figures 2c** and **3a**. The heights of microfibrils ranged typically from 0.5 to 3 nm, although a height profile example is not shown here. These microfibrils are considered to be fragments of larger network-like assemblies (e.g., **Figure 2a**) and produced by heat-induced dissociation of hydrogen bonds among molecules comprising the assemblies. Another type of observed structures was densely cross-linked microgels (**Figure 5**). Because the Curdlan sample used in this study did not form a bulk gel in the examined condition, these are considered to result from localized aggregation. Nevertheless, the area covered by some microgels exceeded the maximum maneuverable range of the scanner (approximately 20 μm × 20 μm) (not shown), indicating that these are indeed precursors of a bulk gel. The driving force of cross-linking reactions in the present case should be heat-induced hydrophobic interactions that are possible among various species in the present system. A free end of a partially dissociated single chain that has the other end still woven into a microfibril may associate with another free end of a partially dissociated chain or even directly with another microfibril. It is also possible that such partially dissociated single chains newly generate triple-stranded helices that play a role as a cross-linker. Additionally, bundles of microfibrils aligned in parallel can be seen in **Figure 5b**, indicating the existence of hydrophobic patches on the surface of microfibrils. The thickness of microfibrils shown in **Figure 5a** appears to be thinner than that shown in **Figure 2c** or **4**. This can be explained if Curdlan molecules in dried powders are already in the form of entangled supramolecular microfibrils and dissociate on heating in an aqueous medium yet to a limited extent, and then these dissociated molecules reassociate via hydrophobic interactions. It should be stressed here, however, that the width of structures in an AFM image is influenced by an effect known as probe-broadening and that the level of broadening depends on various factors such as the shape or size of the tip and the roughness of the sample (*22*). In the case of individual polymer chains spread on the mica surface, the width normally appears 10 times or more larger than that predicted on the basis of the known molecular diameter, whereas recorded heights that are free from probe-broadening can be used as a reasonable measure of the molecular size (*25*−*27*). In the case of thick samples such as microgels and bulk gels (*27*), however, the height of individual fibrils is difficult to evaluate due to difficulties in determining the base plane of each individual fibril.

The present results suggest that heat-induced Curdlan gel networks can be regarded as networks of partially dissociated microfibrils that are cross-linked by newly developed triple helices, associated single helices, and directly associated parts of microfibrils. Unassociated single chains and partially opened triple helices (*33*) are also likely to exist because of topological obstruction in intermolecular association and are expected to contribute mainly to viscous characteristics of a heat-induced gel. On the other hand, the stiffness and the degree of branching of microfibrils are considered to be critical factors for determining the elastic properties of a Curdlan gel. A similar structural model, except for the cross-linking mechanism, has been proposed for cold-setting gels prepared from double-stranded helix-forming polysaccharides, such as agarose, carrageenans, and gellan (*25*, *27*, *34*, *35*). This model has been designated the fibrous model because the gel network is entirely composed of branched fibrous aggregates of double helices (*25*, *27*, *34*, *35*). It is preferable to validate the present results against AFM images of bulk gels. Our attempts at imaging heat-induced bulk gels of Curdlan were, however, unsuccessful. AFM imaging of a bulk gel of polysaccharide has succeeded only in limited cases (*27*, *35*) because the bulk gel surface easily deforms on contact with the probe during imaging. Further technical developments for minimizing the contact force are needed to truly substantiate

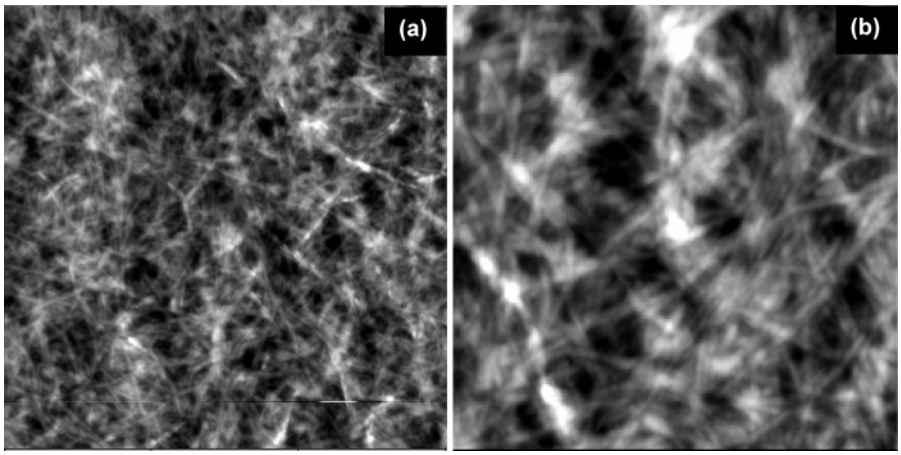

Figure 5. Topographical images of heat-induced Curdlan microgel. Curdlan was first dissolved into 0.01 mol/L NaOH to be 1% w/w, heated at 90 °C for 4 h, diluted into distilled water to be 0.2 mg/mL, and deposited onto mica: (**a**) image size is 2.5 μm × 2.5 μm; (**b**) image size is 1.2 μm × 1.2 μm.

the proposed heat-induced gelation mechanism of Curdlan. Such advanced technology will also allow us to test the generality of the model with special attention to thermodynamic and kinetic parameters depending on both temperature and solvent conditions.

In conclusion, the high-resolution AFM images of molecular assemblies of Curdlan obtained in this study provide the first direct evidence for their structural heterogeneity, suggesting that heat-induced gelation of this polysaccharide involves two steps. Curdlan molecules in the commercially prepared powder sample are suggested to be in the form of entangled microfibrils that are predominantly composed of laterally associated single helices and chains and a relatively small number of triple helices. Such microfibrils were difficult to completely dissociate into individual molecules even in the presence of 1 mol/L NaOH. It is thus considered that the first step of heat-induced gelation of Curdlan suspended in water is to release single molecular chains from microfibrils. Some of these single chains are not completely dissociated: they have one free end in the medium, but the other end is still trapped in a microfibril. These partially dissociated single chains are presumably capable of cross-linking the parent microfibrils through the formation of triple-stranded helices, by hydrophobic association between multiple single helices, and by association between a single helix and microfibril. Direct lateral association between microfibrils also appeared to be involved. Consequently, heat-induced gel networks of Curdlan can be regarded as networks of supramolecular microfibrils cross-linked by triple helices and associated single helices and microfibrils. This structural model shares a common feature with the so-called fibrous model developed for cold-set gels of double-stranded helix-forming polysaccharides (*25*, *34*, *35*) in the sense that the gel network is predominantly composed of microfibrillar aggregates at the supramolecular level.

LITERATURE CITED

(1) Morris, V. J. Gelation of polysaccharides. In *Functional Properties of Food Macromolecules*, 2nd ed.; Hill, S. E., Ledward, D. A., Mitchell, J. R., Eds.; Aspen Publishers: Gaithersburg, MD, 1998; pp 143−226.

(2) Desbrières, J.; Hirrien, M.; Ross-Murphy, S. B. Thermogelation of methylcellulose: rheological considerations. *Polymers* **2000**, *41*, 2451−2461.

(3) Shirakawa, M.; Yamatoya, K.; Nishinari, K. Tailoring of xyloglucan properties using an enzyme. *Food Hydrocolloids* **1998**, *12*, 25−28.

(4) Tada, T.; Matsumoto, T.; Masuda, T. Influence of alkaline concentration on molecular association structure and viscoelastic properties of Curdlan aqueous systems. *Biopolymers* **1997**, *42*, 479−487.

(5) Tada, T.; Matsumoto, T.; Masuda, T. Dynamic viscoelasticity and small-angle X-ray scattering studies on the gelation mechanism and network structure of Curdlan gels. *Carbohydr. Polym.* **1999**, *39*, 53−59.

(6) Funami, T.; Funami, M.; Yada, H.; Nakao, Y. A rheological study on the effects of heating rate and dispersing method on the gelling characteristics of Curdlan aqueous dispersions. *Food Hydrocolloids* **2000**, *14*, 509−518.

(7) Zhang, H.; Nishinari, K.; Williams, M. A. K.; Foster, T. J.; Norton, I. T. A molecular description of the gelation mechanism of Curdlan. *Int. J. Biol. Macromol.* **2002**, *30*, 7−16.

(8) Saitô, H.; Yoshioka, S.; Uehara, N.; Aketagawa, J.; Tanaka, S.; Shibata, Y. Relationship between conformation and biological response for (1→3)-*β*-D-glucans in the activation of coagulation Factor G from limulus amebocyte lysate and host-mediated antitumor activity. Demonstration of single-helix conformation as a stimulant. *Carbohydr. Res.* **1991**, *217*, 181−190.

(9) Kulicke, W.-M.; Lettau, A. I.; Thielking, H. Correlation between immunological activity, molar mass, and molecular structure of different (1→3)-*β*-D-glucans. *Carbohydr. Res.* **1997**, *297*, 135−143.

(10) Kataoka, K.; Muta, T.; Yamazaki, S.; Takeshige, K. Activation of macrophages by linear (1→3)-*β*-D-glucans. *J. Biol. Chem.* **2002**, *27*, 36825−36831.

(11) Konno, A.; Harada, T. Thermal properties of Curdlan in aqueous suspension and Curdlan gel. *Food Hydrocolloids* **1991**, *5*, 427−434.

(12) Nakao, Y.; Konno, A.; Taguchi, T.; Tawada, T.; Kasai, H.; Toda, J.; Terasaki, M. Curdlan—properties and application to foods. *J. Food Sci.* **1991**, *56*, 769−772, 776.

(13) Deslandes, Y.; Marchessault, R. H.; Sarko, A. Triple-helical structure of (1→3)-*β*-D-glucan. *Macromolecules* **1980**, *13*, 1466−1471.

(14) Saitô, H. Conformation and dynamics of (1→3)-*β*-D-glucans in the solid and gel state. *ACS Symp. Ser.* **1992**, *No. 489*, 296−310.

(15) Nakata, M.; Kawaguchi, T.; Kodama, Y.; Konno, A. Characterization of Curdlan in aqueous sodium hydroxide. *Polymers* **1998**, *39*, 1475−1481.

(16) Futatsuyama, H.; Yui, T.; Ogawa, K. Viscometry of Curdlan, a linear (1→3)-*β*-D-glucan, in DMSO or alkaline solutions. *Biosci., Biotechnol., Biochem.* **1999**, *63*, 1481−1483.

(17) Koreeda, A.; Harada, T.; Ogawa, K.; Sato, S.; Kasai, N. Study of the ultrastructure of gel-forming (1→3)-*β*-D-glucan (curdlan-type polysaccharide) by electron microscopy. *Carbohydr. Res.* **1974**, *33*, 396−399.

(18) Harada, T.; Koreeda, A.; Sato, S.; Kasai, N. Electron microscopic study on the ultrastructure of Curdlan gel: assembly and dissociation of fibrils by heating. *J. Electron Microsc.* **1979**, *28*, 147−153.

(19) Takahashi, F.; Harada, T.; Koreeda, A.; Harada, A. Structure of Curdlan that is resistant to (1→3)*β*-D-glucanase. *Carbohydr. Polym.* **1986**, *6*, 407−421.

(20) Kanzawa, Y.; Harada, T.; Koreeda, A.; Harada, A.; Okuyama, K. Difference of molecular association in two types of Curdlan gel. *Carbohydr. Polym.* **1989**, *10*, 299−313.

(21) Harada, T.; Kanzawa, Y.; Kanenaga, K.; Koreeda, A.; Harada, A. Electron microscopic studies on the ultrastructure of Curdlan and other polysaccharides in gels used in foods. *Food Struct.* **1991**, *10*, 1−18.

(22) Morris, V. J.; Kirby, A. R.; Gunning, A. P. *Atomic Force Microscopy for Biologists*; Imperial College Press: London, U.K., 1999.

(23) Morris, V. J.; Mackie, A. R.; Wilde, P. J.; Kirby, A. R.; Mills, E. C. N.; Gunning, A. P. Atomic force microscopy as a tool for interpreting the rheology of food biopolymers at the molecular level. *Lebensm.-Wiss. -Technol.* **2001**, *34*, 3−10.

(24) Ikeda, S.; Morris, V. J. Fine-stranded and particulate aggregates of heat-denatured whey proteins visualized by atomic force microscopy. *Biomacromolecules* **2002**, *3*, 382−389.

(25) Ikeda, S.; Morris, V. J.; Nishinari, K. Microstructure of aggregated and nonaggregated *κ*-carrageenan helices visualized by atomic force microscopy. *Biomacromolecules* **2001**, *2*, 1331−1337.

(26) Ikeda, S.; Nitta, Y.; Kim, B. S.; Temsiripong, T.; Pongsawatmanit, R.; Nishinari, K. Single-phase mixed gels of xyloglucan and gellan. *Food Hydrocolloids* **2004**, *18*, 669−675.

(27) Ikeda, S.; Nitta, Y.; Temsiripong, T.; Pongsawatmanit, R.; Nishinari, K. Atomic force microscopy studies on cation-induced network formation of gellan. *Food Hydrocolloids* **2004**, *18*, 727−735.

(28) Ogawa, K.; Tsurugi, J.; Watanabe, T. Complex of gel-forming *β*-1,3-D-glucan with congored in alkaline solution. *Chem. Lett.* **1972**, 689−692.

(29) Ogawa, K.; Tsurugi, J.; Watanabe, T. The dependence of the conformation of a (1→3)-*β*-D-glucan on chain-length in alkaline solution. *Carbohydr. Res.* **1973**, *29*, 397−403.

(30) Ogawa, K.; Hatano, M. Circular dichroism of the complex of a (1→3)-β-D-glucan with Congo Red. *Carbohydr. Res.* **1978**, *67*, 527−535.
(31) Ogawa, K.; Dohmaru, T.; Yui, T. Dependence of complex formation of (1→3)-β-D-glucan with Congo Red on temperature in alkaline solution. *Biosci., Biotechnol., Biochem.* **1994**, *58*, 1870−1872.
(32) Yang, J.; Mou, J.; Shao, Z. Molecular resolution atomic force microscopy of soluble proteins in solution. *Biochim. Biophys. Acta* **1994**, *1199*, 105−114.
(33) Young, S.-H.; Dong, W.-J.; Jacobs, R. R. Observation of a partially opened triple-helix conformation in 1→3-β-glucan by fluorescence resonance energy transfer spectroscopy. *J. Biol. Chem.* **2000**, *275*, 11874−11879.
(34) Gunning, A. P.; Morris, V. J. Light scattering studies of tetramethylammonium gellan. *Int. J. Biol. Macromol.* **1990**, *12*, 338−341.
(35) Gunning, A. P.; Kirby, A. R.; Ridout, M. J.; Brownsey, G. J.; Morris, V. J. Investigation of gellan networks and gels by atomic force microscopy. *Macromolecules* **1996**, *21*, 6791−6796.

Received for review July 19, 2004. Revised manuscript received November 4, 2004. Accepted November 24, 2004.

JF048797R